Dalton
Transactions

Accepted Manuscript

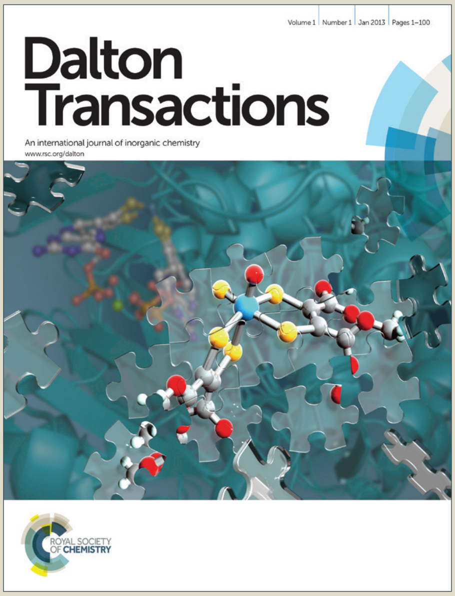

ROYAL SOCIETY
OF CHEMISTRY

www.rsc.org/dalton

Dalton Transactions

Dynamic Article Links ►

Cite this: DOI: 10.1039/c0xx00000x

www.rsc.org/xxxxxx

PAPER

Efficient visible and near-infrared photoluminescent attapulgite-based lanthanide one-dimensional nanomaterials assembled by ion-pairing interactions

Jun Xu,[a,b] Ye Zhang,[a] Hao Chen,[a] Weisheng Liu[a] and Yu Tang*[a]

Received (in XXX, XXX) Xth XXXXXXXXX 20XX, Accepted Xth XXXXXXXXX 20XX
DOI: 10.1039/b000000x

Attapulgite, a one-dimensional fibrillar nanomaterial present in nature, with its extreme stabilities, is promising to act as a new carrier of luminescent lanthanide complexes for the further applications. Herein, a series of lanthanide complexes Na[Ln(TTA)$_4$] have been attached to attapulgite (Atta) via ion-pairing interactions, generating the first example of attapulgite-based visible and near-infrared (NIR) luminescent lanthanide one-dimensional nanomaterials, where TTA is 2-thenoyltrifluoroacetonate and Ln is Eu, Sm, Nd, Er or Yb. The hybrid materials were characterized by CHN elemental analysis, inductively coupled plasma-atomic emission spectroscopy (ICP), powder X-ray diffraction (PXRD), thermogravimetry (TG), transmission electron microscopy (TEM), and UV-vis absorption spectra. In order to investigate the photophysical behaviours of these materials, the visible and NIR luminescent spectra and the energy transfer process have been systematically investigated. Moreover, efforts have been made to Eu- and Sm-based plastic attapulgite materials by utilizing the poly(methyl methacrylate) (PMMA) matrices, and the dispersibility of lanthanide doped hybrids in the PMMA provides them high mechanical strength. The lanthanide-doped attapulgite appears to be an interesting material for photophysical applications. The results of this work would have potential significance for the design and assembly of the luminescent lanthanide materials for light-emitting diodes (LED), sunlight-conversion film, optical amplifiers, solar concentrators, and lasers.

Introduction

Lanthanide ions exhibits specific, line-shape f-f emissions, covering a large spectroscopic range from visible to near-infrared (NIR), for instance, with orange for Sm(III), red for Eu(III), green for Tb(III), yellow for Dy(III) and NIR for Sm(III), Nd(III), Er(III) and Yb(III), which are suitable for various applications, such as lighting,[1] lasers,[2] up-conversion[3] and bio-imaging.[4] Lanthanide ions exhibit, however, low luminescence intensity due to the fact that the 4f-4f transitions are parity forbidden. One of the most useful strategies that has been employed to overcome this drawback is the complexation of the lanthanide ions through the coordination with organic ligands acting as antenna or sensitizers, which could absorb the excitation light energy and transfer the energy from its lowest triplet state energy level (T$_1$) to the resonance level of lanthanides.[5] Furthermore, the complexation with a ligand provides lanthanides with a certain degree of protection from the solvent molecules, hence, increasing their luminescence quantum yields. β-Diketonate lanthanide complexes are the most popular and intensively investigated luminescent lanthanide complexes,[6] because of the relatively easy synthesis and the excellent luminescent properties.

Unfortunately, isolated lanthanide complexes have been excluded from wider practical applications due to their poor stabilities under high temperature, moisture conditions and UV light.[7] By incorporating luminescent lanthanide complexes into the matrices, the obtained hybrids could show superior chemical and optical properties, including high stabilities and long luminescence lifetimes, as well as high resistance to photobleaching.[8] Among many candidates, attapulgite (so-called palygorskite) are certainly suitable scaffolding materials due to their excellent properties. Attapulgite (Atta) is a hydrated magnesium aluminium silicate present in nature as a one-dimensional fibrillar silicate clay mineral, with large specific surface area and pronounced adsorption properties.[9] It is famous for Maya blue,[10] a nanocomposite combining attapulgite with indigo dye, which has confounded researchers for its extreme chemical stability and remarkable exposure durability for decades.[11] Combining luminescent lanthanide complexes with attapulgite, to improve their stabilities and even luminescent properties is fascinating, promising but challenging in the field of lanthanide hybrids.

Our group is dedicated to the design and assembly of Atta-based materials covalently bonded with lanthanide complexes.[12] Herein, we describe the design and assembly of a series of Atta-based, visible and NIR lanthanide luminescent one-dimensional nanomaterials. The lanthanide complexes are non-covalently adsorbed on the surface of attapulgite through strong electrostatic interactions, different from the previous approach (Scheme 1). Actually, a negatively charged Ln(III) complex Nan[Ln(TTA)$_4$] (Ln= Eu, Sm, Nd, Er or Yb) is adsorbed onto Atta coated with a positively charged imidazolium ionic liquid (IL). Ionic liquids can be thoroughly dried due to their low vapor pressure, so that the water concentration can be lowered to a very low level. This is an advantage for the lanthanide(III) emission, because water molecules in the neighborhood of the lanthanide ion can quench the excited states. Moreover, ionic liquids can exhibit useful properties such as electric conductivity and a high thermal and electrochemical stability.[13] In the ionic liquid doped lanthanide materials, the coordination sphere of the lanthanide ion is saturated by the ligands and thus no solvent coordination occurs. So the ionic liquid are attractive media for visible and NIR luminescence, and may participate in the sensitization process.[14] In order to investigate the photophysical behaviors of these materials, the visible and NIR luminescent properties, including the luminescence spectra and lifetimes have been systematically investigated in our study. In the present work, efforts have also been made to Eu- and Sm-based plastic materials by combining the unique optical properties of Eu-based hybrid material (**4a**) and Sm-based material (**4b**) with the mechanical characteristics, thermal stability, flexibility and film-forming tendency of polymer poly(methyl methacrylate) (PMMA). The high dispersibility of material **4a** and **4b** in a polymer matrix (PMMA) make them as promising luminophores for applications in sunlight-conversion film, polymer optical fibers as well as light emitting devices.

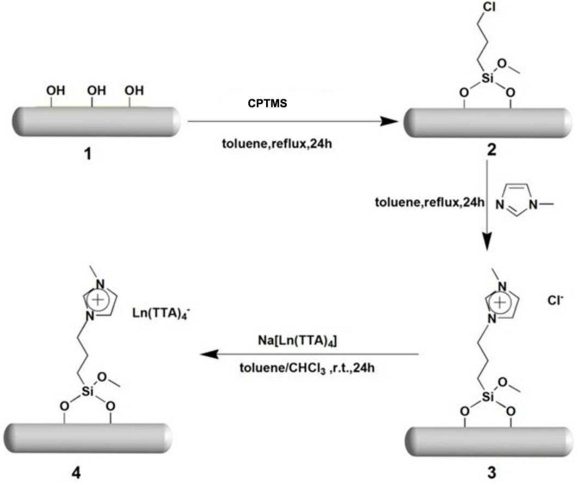

Scheme 1 The assemble procedure of the lanthanide hybrid materials.

Results and Discussion

Characterization of Microstructure

The FTIR spectra of the materials **1**, **2**, **3**, and **4a** are shown in Fig. S1. As shown in the FTIR spectrum of material **3**, the characteristic absorbance for the C=N bonds of an imidazole ring is found at 1570 cm^{-1}, suggesting that 1-methylimidazole has been successfully immobilized onto the surface of Atta. However, it is of little possibility to predict the forms of the Eu-doped material (**4a**) in the FTIR spectrum. This is because the amount of the complexes incorporated in the matrix is low, and the peak of Si-O-Si framework vibrations (ν_{as}(Si-O-Si) at 1086 cm^{-1}, and δ(Si-O-Si) at 462 cm^{-1}) and stretching vibrations of physically absorbed water at 1633 cm^{-1} are strong relatively.

The chemical compositions of the hybrid materials **2**, **3**, and **4a-e** were compiled in Table S1. Elemental analysis indicated the carbon content of material **2** is 6.04%, which translates to a chloropropylsilyl loading of about 1.26 mmol g^{-1} through that the chloropropylsilyl groups are anchored to the surface by two methoxy group, with one residual methoxy group per Si atom. After functionalization by the imidazolium, the nitrogen content in material **3** was 3.01%, corresponding to about 1.07 mmol of imidazolium per gram of the material. The Eu content in material **4a** was 1.85% tested by ICP, corresponding to 0.12 mmol of complexes per gram of material. And other Ln contents in materials **4b-e** are the same as that of Eu as listed in Table S1. These results emphasized that the lanthanide complex could bonded to Atta matrix through this ion-pairing interaction. However, the hindrance of the complex limits the process of grafting, resulting the lower grafting ratios.[15]

The TGA curves of the hybrid materials **2**, **3**, and **4a** were listed in Fig. S2. In each case, the first weight loss in the temperature range 80-180 °C can be ascribed to water desorption as an endothermic process. Further heating shows a weight loss as an exothermic process at 200-600 °C. Compared with the thermal behavior of material **2**, decomposition of the organic moieties in material **3** occurs over a slightly wider range and consists of two well-defined steps centred at 220 and 380 °C. The weight loss of the organic moieties was 25.6% corresponding to 1.1 mmol g^{-1} between 200 and 600 °C, which is in good agreement with the grafting ratios computed from elemental analysis. And TGA of material **4a** shows a weight loss of 27.3%, corresponding to the organic moieties decomposition.

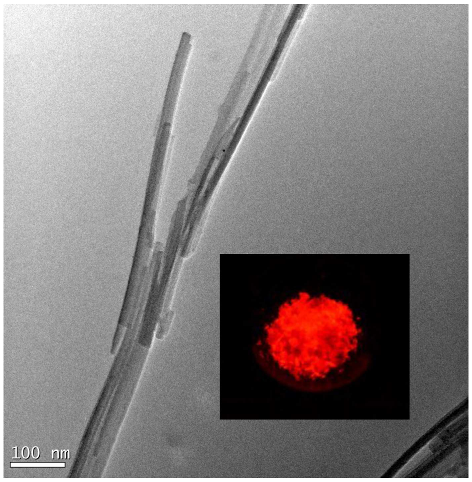

Fig. 1 The measured Transmission Electron Microscopy (TEM) image of the material **4a.** The inset photograph shows the material **4a** under UVA irradiation (365 nm).

The PXRD analyses of the materials **1**, **2**, **3**, and **4a** are shown in Fig. S3, respectively. After grafting, the peak positions (2θ) at 8.4°, 19.8°, 26.6°, 34.9°, and 42.3° are exactly the same as in pure Atta, which indicates the structure of the attapulgite is maintained and the interaction occurred on the surface but not in the interlayer. However, the peaks at 13.6° and 16.2° correspond to the Si–O–Si crystalline layer were strongly reduced in materials **2**, **3**, and **4a**, indicating that the complex has been grafted on Atta surfaces successfully.

The measured Transmission Electron Microscopy (TEM) image of the material **4a** (Fig. 1) revealed that the structure maintained inhomogenous rodlike morphology derived from natural substrates after forming the hybrids.

The absorption spectra of materials **2**, **3**, and **4a** are displayed in Fig. 2. The material **2** displayed a strong and relatively sharp absorption band at 218 nm. After functionalization by the imidazolium (material **3**), the absorption band of the material at 218 nm began to weaken and the material showed a wide absorption band centered at 250 nm, which can be attributed to the π-π* transitions of the imidazole. A wide absorption band at 320-400 nm corresponding to π-π* transitions of the ligand TTA^- in material **4a** is observed, indicating that the complex is loaded on the Atta matrix.

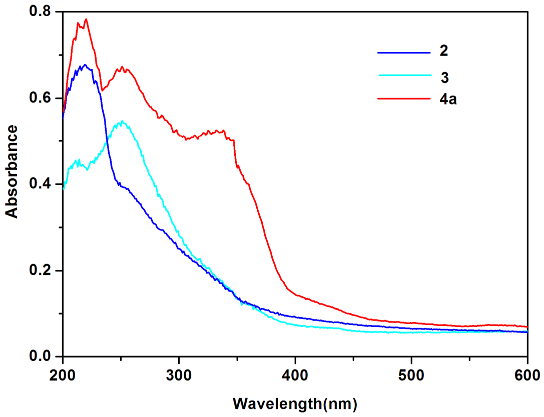

Fig. 2 Solid-state absorption spectra of the hybrid materials **2**, **3**, and **4a**.

Luminescent Properties Analyses for the Hybrid Materials.

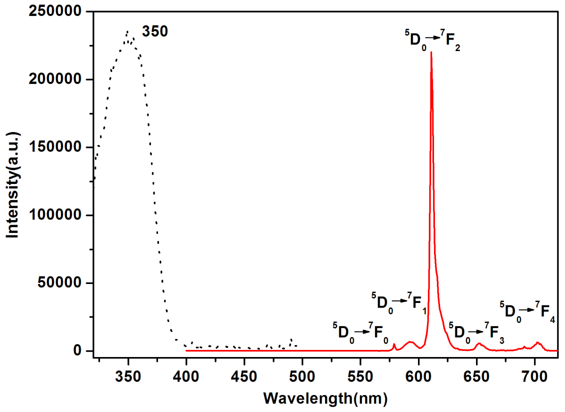

Fig. 3 Excitation (left) and emission spectra (right) of the hybrid material **4a**.

Having assessed that the lanthanide complexes are tightly bound onto the surface of the Atta, we have investigated the photophysical properties of the hybrid materials, in particular their luminescence performance. The bright red light emissions under UVA (365 nm) irradiation can be observed in the Eu-doped hybrid material **4a** (Fig. 1). It is illustrated in Fig. 3 the excitation (left) and emission (right) spectra of hybrid material **4a** at room temperature. The excitation spectrum which is monitored with $^5D_0\rightarrow{}^7F_2$ transition at 612 nm of Eu(III) for the sample, exhibit a broad excitation band (BEB) between 300 and 420 nm, which can be assigned to the π-π* electron transition of the ligand TTA^-. Fig. S4 shows the room temperature excitation spectra of the materials **4b-e**. All of the spectra also display a large broad band ascribed to the excited states of the ligand TTA^-, which indicates that the ligand can be a good organic chelator to absorb energy and transfer it to lanthanide ions even after the lanthanide complexes are tightly bound onto the surface of the Atta. In the emission spectrum of the sample **4a**, only characteristic emission of Eu^{3+} arising from the transition $^5D_0\rightarrow{}^7F_J$ (J = 0, 1, 2, 3, 4) is detected with the transition $^5D_0\rightarrow{}^7F_2$ red emission as the dominant group, which indicates that an efficient energy transfer from the ligands to Eu^{3+} emitting center by the antenna effect can take place in the Eu-doped hybrid material. The quantum yield of the material **4a** is 12.81%, which is determined by employing an integrating sphere.

Although the red emission by Sm(III) is less intense than that of Eu(III) and shifted further to the near-infrared region, the Sm(III) ion is of interest because the emission range can cover the visible as well as the near-infrared part. However, most luminescence studies on Sm(III) complexes neglect the near-infrared emission of this lanthanide ion. Only recently, near-infrared emission by Sm(III) in molecular complexes is receiving more attention.[16] The spectrum of the Sm-doped hybrid material **4b** was recorded at room temperature (Fig. 4a), and the emission range covers the visible and the near-infrared region. All of the narrow peaks observed in the luminescence emission spectrum of Sm(III) are transitions between the $^4G_{5/2}$ excited state and the different J-levels of the ^6H term (^6H_J, J = 5/2-15/2) and the ^6F term (^6F_J, J = 1/2-9/2). The most intense transition in the visible region is the hypersensitive $^4G_{5/2}\rightarrow{}^6H_{9/2}$ line at 643 nm, and the quantum yield of the material **4b** is 2.64%. This wavelength is consistent with the absorbing wavelength of chlorophyll B, which means the efficiency of photosynthesis can be optimized and the crop yield can be improved when the unused portions of the solar spectrum are converted. In the near-infrared area, the most intense transition is $^4G_{5/2}\rightarrow{}^6F_{5/2}$ line at 948 nm.

The Nd^{3+}-doped materials have been regarded as the most popular near-infrared luminescence materials since they are available in the field of laser systems.[17] The emission spectrum of the Nd-doped hybrid **4c** exhibited three bands (Fig. 4b) including 906 nm ($^4F_{3/2}\rightarrow{}^4I_{9/2}$), 1062 nm ($^4F_{3/2}\rightarrow{}^4I_{11/2}$), and 1335 nm ($^4F_{3/2}\rightarrow{}^4I_{13/2}$), respectively. The strongest emission is centered at around 1062 nm (Fig. S5), which is served as the well known transition used in lasers. In addition, the bands at 1335 nm of the Nd hybrid materials will offer the opportunity for application in optical amplifiers.[18]

Recently, the urgent demand for optical amplifiers with a wide and flat gain spectrum in the telecommunication window has emerged upon the increasing of information capacity. The Er^{3+} ion is of interest for use as an optical amplifier, due to its standard telecommunication wavelength at about 1500 nm.[19] When the Er-doped hybrid material **4d** was excited at 360 nm, a large emission range from 1450 to 1625 nm centered at 1541 nm can be monitored (Fig. 4c), which is attributed to the transition from the first excited state ($^4I_{13/2}$) to the ground state ($^4I_{15/2}$) of the Er^{3+} ion (Fig. S5). The full width at half maximum (FWHM) of the emission of Er^{3+} ion, which is an important parameter for potential application in the telecommunication area, has also been determined. The Er-doped hybrid material **4d** showed a relative broad band and the FWHM was 84 nm, which may enable a wide gain bandwidth for optical amplification.[20]

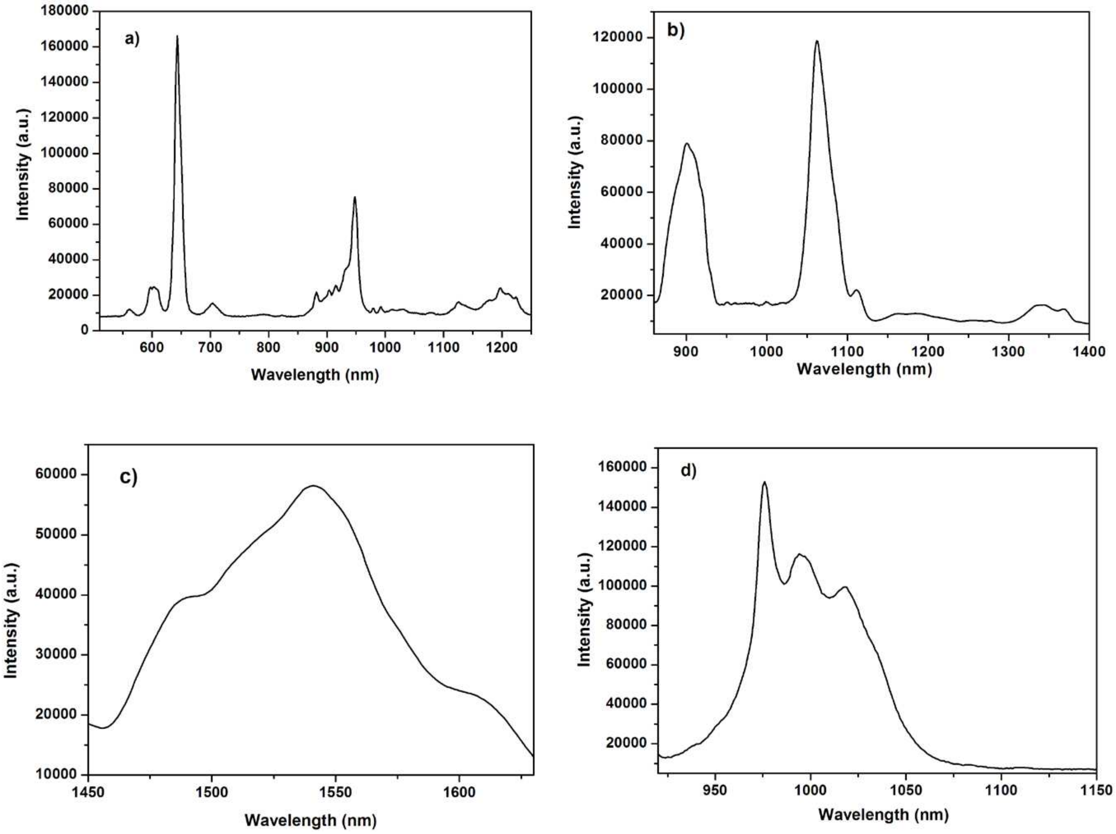

Fig. 4 Emission spectra of the hybrid materials: (a) **4b**, (b) **4c**, (c) **4d**, and (d) **4e**.

For the emission spectrum of the Yb-doped hybrid **4e**, a band in the range of 925-1100 nm with the strongest peak at 978 nm was detected, which can be assigned to the $^2F_{5/2}\rightarrow{}^2F_{7/2}$ transition of the central Yb^{3+} ion (Fig. 4d). It should also be noted that the emission band of the Yb^{3+} ion is not a single sharp band but a shoulder peak arising at long wavelength than the primary 978 nm band, which results from the crystal field splitting.[21] In the field of the laser materials, the Yb-doped hybrid plays an important role due to its simple energy levels. The intense emission of Yb^{3+} ion will be well suited for laser diode pumping in this range and the smaller Stokes shift between absorption and emission reduces the thermal loading of the material during laser operation.[22] Additionally, the relative transparency of human tissue at approximately 1000 nm makes it as a promising probe for fluoroimmuno-assays and vivo applications.[23]

To help understand the observed spectral results, all the major energy transfer during the sensitization of lanthanide luminescence via the ligand TTA^- and primary energy levels involved were illustrated in Fig. S5. Because no transitions of the lanthanide ions occur in the excitation spectra (Fig. 3 and Fig. S4), the observed vis/NIR emission can only originate from the lanthanide ions sensitized by the ligands moiety. The obtained visible or near-infrared photoluminescence in this case illustrates that the ligands can shield the lanthanide ions well from the surroundings and the intramolecular energy transfer does occur between the ligands and the lanthanide ions by the antenna effect.

The luminescence lifetimes of the materials **4a-e** in the solid-state are shown in Table S2. The luminescence decays of all the materials can be fitted by bi-exponential functions, indicating that more than one kind of symmetrical site of Ln^{3+} ion exists in these solid samples, which is attributable to site-to-site heterogeneity in the solid state.[24] Since the multiexponential decay curves which are usually observed in the solid hybrids,[25] the average lifetime $<\tau>$ can be calculated using the following equation (1)

$$<\tau>=\frac{\sum A_i\tau_i^2}{\sum A_i\tau_i} \qquad (1)$$

Where τ_i is the component decay times and A_i is the preexponential factors related to the statistical weights of each exponential. The luminescence decay times of these materials are the same as ionic-liquid lanthanide complexes $[C_6mim][Ln(TTA)_4]$ reported in the previous reference,[26] which means that the effective intermolecular transfer systems have been accomplished in the materials even though the contents of the lanthanide were very low in the hybrids. The results may also support the conclusion that the O-H groups could not act as efficient outer sphere oscillators to quench the NIR emission and the nanoconfinement of the ionic liquid in the matrix does not disturb the first coordination sphere of the lanthanide ions.

The Eu-doped and Sm-doped Plastic Materials

Lanthanide-doped hybrid materials are known to be efficiently incorporated in many types of optically transparent polymeric matrices, such as poly(methyl methacrylate) (PMMA),[27] poly(vinyl pyrrolidone) (PVP)[28] and polystyrene (PS),[29] affording interesting materials for possible application in organic light-emitting diodes (OLEDs) and luminescent fibers.[30] In the present work, we decided to perform the Eu-doped and Sm-doped plastic materials by employing materials **4a** and **4b** in the polymer PMMA, which own the mechanical characteristics, thermal stability, flexibility, and film-forming tendency. The resulting polymeric composites are well dispersed, flexible, and show a bright red or orange luminescence typical of Eu(III) or Sm(III) ions upon irradiation at 365 nm. Fig. 5 shows the photograph of the polymer composite films under day light and UV light (365 nm). It can be found that the emissions of the films are powerful even at very low quality percentages of materials **4a** and **4b**. More likely, these materials could provide excellent photophysical properties and low cost for practical application.

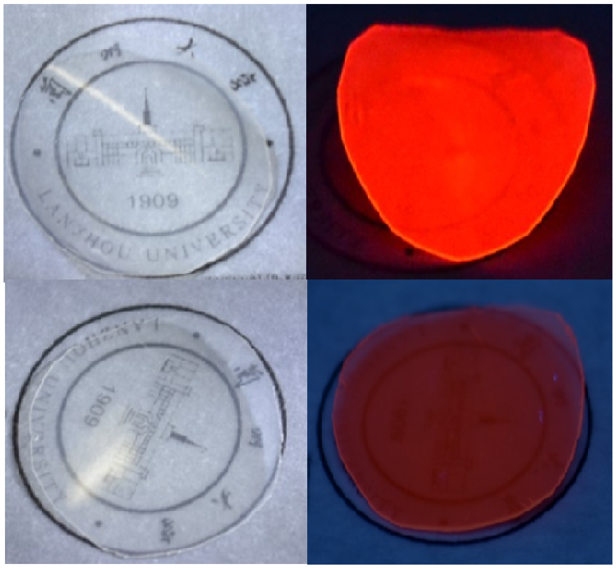

Fig. 5 Pictures of the Eu-doped plastic material (top) and Sm-doped plastic material (down).

Conclusions

In this paper we have reported one-dimensional attapulgite-based lanthanide hybrid nanomaterials, in which the attapulgite scaffold is buried in a positively charged group, which is ion-paired with a negatively charged lanthanide complexes, Na[Ln(TTA)$_4$] (Ln = Eu, Sm, Nd, Er or Yb). These materials display efficient visible or near-infrared photoluminescence. Thanks to the high loading of the emissive species and the unchanged luminescence performances of the resulting hybrid materials after dispersed in polymer matrix, these materials would have potential significance for the design and assembly of the luminescent lanthanide materials for light-emitting diodes (LED), sunlight-conversion film, optical amplifiers, and medical diagnostic probe.

Experimental Section

Materials

(3-Chloropropyl)-trimethoxysilane (CPTMS, 99%) was reagent of Acros Organics. Samarium ($SmCl_3{\cdot}6H_2O$), europium ($EuCl_3{\cdot}6H_2O$), neodymium ($NdCl_3{\cdot}6H_2O$), erbium ($ErCl_3{\cdot}6H_2O$) and ytterbium chlorides ($YbCl_3{\cdot}6H_2O$) were obtained by dissolving Sm_2O_3, Eu_2O_3, Nd_2O_3, Er_2O_3 and Yb_2O_3 (99.99%, Shanghai Yuelong) in hydrochloric acid followed by successive fuming to remove excess acid, respectively. 2-Thenoyltrifluoroacetone (HTTA, AR) and 1-methylimidazole were all commercially available and used as received. Attapulgite (Atta, Jiangsu Autobang Co. Ltd., China) was purified through dispersion into $(NaPO_3)_6$ aqueous solutions, followed by treating with HCl and H_2O_2. All the other reagents are analytical pure and purchased from China National Medicines Group.

Synthesis of Chloropropylsilyl Groups Functionalized Atta (2)

As described in Scheme 1, an excess of (3-chloropropyl)-trimethoxysilane (CPTMS) (1mL) was added to a suspension of the dry Atta (500 mg) in toluene (50 mL), and the mixture was stirred under reflux for 8 h. The solid was then separated by centrifugation, washed with CH_2Cl_2 (3× 30 mL), and dried under reduced pressure at room temperature.

Synthetic Procedure of Atta Containing Immobilized 1-Propyl-3-methylimidazolium Chloride Groups (3)

Samples of material **2** (500 mg) and an excess of 1-methylimidazole (1 mL) were suspended in toluene (30 mL), sonicated for 30 min, and then stirred under reflux for 24 h and centrifuged. Through washing the resulting solids with CH_2Cl_2 (3× 30 mL) and drying at room temperature, the 1-propyl-3-methylimidazolium chloride groups functionalized sample was obtained.

Synthesis of 1-Propyl-3-methylimidazolium Tetrakis(2-thenoyltrifluoroacetone) Lanthanide(III) Groups Functionalized Atta (4)

To obtain the material **4**, the lanthanide complexes (Na[Ln(TTA)$_4$]) should be firstly synthesized by using a literature procedure.[6a] For Na[Eu(TTA)$_4$], typically: 0.444 g of HTTA (2 mmol) is dissolved in ethanol (10 mL) and deprotonated with 1 M NaOH (2 mL) at room temperature. A suspension of $EuCl_3{\cdot}6H_2O$ (0.23 g, 0.05 mmol) in EtOH (5 mL) was then added slowly and the mixture stirred for 4 h at 50 °C. The solvent was removed under reduced pressure and the resultant yellow product washed with diethyl ether and n-hexane. The product was dissolved in $CHCl_3$ (10 mL) and added to a suspension of material **3** (0.25 g) in toluene (25 mL). After stirring the mixture at room temperature for 24 h, the resultant powder was filtered and washed with $CHCl_3$ (3×20 mL), deionized water (20 mL), ethanol (2×20 mL), diethyl ether (20 mL). After drying under reduced pressure at room temperature for several hours, Eu-doped hybrid material (**4a**) was obtained. The synthesis procedures for Na[Sm(TTA)$_4$], Na[Nd(TTA)$_4$], Na[Er(TTA)$_4$], and Na[Yb(TTA)$_4$] are similar to that for Na[Eu(TTA)$_4$]. The other hybrid materials **4b**, **4c**, **4d**, and **4e** were prepared as described above for **4a**, using Na[Sm(TTA)$_4$], Na[Nd(TTA)$_4$], Na[Er(TTA)$_4$], and Na[Yb(TTA)$_4$], respectively.

Synthesis of Eu-doped and Sm-doped PMMA Films

Eu-doped and Sm-doped PMMA films were prepared by dispersion of **4a** and **4b** (1 wt %) in PMMA in the solution of tetrahydrofuran, and the resulting composites were heated at 40 °C for 30 min. The polymer films were obtained after the total evaporation of the solvent at 60 °C.

Measurements

CHN elemental analyses were measured on an Elementar Vario EL analyzer; the contents of Ln^{3+} (Ln= Sm, Eu, Nd, Er and Yb) ions were obtained by inductively coupled plasma-atomic emission spectroscopy (ICP) using an IRIS Advantage ER/S spectrophotometer. Fourier transform infrared (FTIR) spectra were conducted within the 4000-400 cm^{-1} wavenumber range using a Nicolet 360 FTIR spectrometer with the KBr pellet technique. Transmission electron microscope (TEM) images were taken on a JEM-1200 EX/S apparatus. Powder X-ray diffraction patterns (PXRD) were determined with Rigaku-Dmax 2400 diffractometer using Cu $K\alpha$ radiation over the 2θ range of 5-70º. The UV-vis absorption spectra were recorded on a Perkin Elmer Lambda 950 spectrophotometer using an integrating sphere. Thermogravimetric analyses (TGA) were performed on a Perkin-Elmer thermal analyzer up to 800°C at a heating rate of $10°C\cdot min^{-1}$ under nitrogen atmosphere. The steady-state luminescence spectra and the lifetime measurements were measured on an Edinburgh Instruments FSL920 fluorescence spectrometer, with a 450 W Xe arc lamp as the steady-state excitation source and a Nd-pumped OPOlette laser as the excitation source for lifetime measurements. Quantum yields of the solid-state samples were determined by an absolute method using an integrating sphere[31] (150mm diameter, $BaSO_4$ coating) on Edinburgh Instrument FLS920.

Acknowledgements

The research leading to these results has received funding from the National Natural Science Foundation of China (Project 21071068, 20931003).

Notes and references

[a] *Key Laboratory of Nonferrous Metal Chemistry and Resources Utilization of Gansu Province, State Key Laboratory of Applied Organic Chemistry and College of Chemistry and Chemical Engineering, Lanzhou University, Lanzhou, 730000 (P. R. China), E-mail: tangyu@lzu.edu.cn. Fax: (+86) 931-891-2582*

[b] *Department of Physics and Chemistry, Henan Polytechnic University, Jiaozuo 454000 (P. R. China)*

† Electronic Supplementary Information (ESI) available: [details of any supplementary information available should be included here]. See DOI: 10.1039/b000000x/

1 (a) D. Parker, R. S. Dickins, H. Puschmann, C. Crossl and J. A. K. Howard, *Chem. Rev.*, 2002, **102**, 1977; (b) S. V. Eliseeva and J. C. G. Bünzli, *Chem. Soc. Rev.*, 2010, **39**, 189; (c) A. D'Aléo, F. Pointillart, L. Ouahab, C. Andraud and O. Maury, *Coord. Chem. Rev.*, 2012, **256**, 1604; (d) J. C. G. Bünzli, *Acc. Chem. Res.*, 2005, **39**, 53; (e) E. G. Moore, A. P. S. Samuel and K. N. Raymond, *Acc. Chem. Res.*, 2009, **42**, 542.

2 (a) K. Binnemans, *Chem. Rev.*, 2009, **109**, 4283; (b) A. P. Bassett, S. W. Magennis, P. B. Glover, D. J. Lewis, N. Spencer, S. Parsons, R. M. Williams, L. De Cola and Z. Pikramenou, *J. Am. Chem. Soc.*, 2004, **126**, 9413.

3 M. Wang, C. Mi, Y. Zhang, J. Liu, F. Li, C. Mao and S. Xu, *J. Phys. Chem. C*, 2009, **113**, 19021.

4 J. Zhang, P. D. Badger, S. J. Geib and S. Petoud, *Angew. Chem., Int. Ed.*, 2005, **44**, 2508.

5 (a) J. C. G. Bünzli and C. Piguet, *Chem. Soc. Rev.*, 2005, **34**, 1048; (b) M. Fernandes, S. S. Nobre, M. C. Gonçalves, A. Charas, J. Morgado, R. A. S. Ferreira, L. D. Carlos and V. de Zea Bermudez, *J. Mater. Chem.*, 2009, **19**, 733; (c) H. Kim and J. Y. Chang, *Soft Matter*, 2011, **7**, 7952.

6 (a) A. M. Klonkowski, S. Lis, M. Pietraszkiewicz, Z. Hnatejko, K. Czarnobaj and M. Elbanowski, *Chem. Mater.*, 2003, **15**, 656; (b) P. A. Vigato, V. Peruzzo and S. Tamburini, *Coord. Chem. Rev.*, 2009, **253**, 1099.

7 (a) C. P. McCoy, *Chem. Mater.*, 2006, **18**, 4336; (b) Q. Li, T. Li and J. G. Wu, *J. Phys. Chem. B*, 2001, **105**, 12293.

8 (a) R. Si, Y. W. Zhang, L. P. You and C. H. Yan, *Angew. Chem., Int. Ed.*, 2005, **44**, 3256; (b) E. H. de Faria, E. J. Nassar, K. J. Ciuffi, M. A. Vicente, R. Trujillano, V. Rives and P. S. Calefi, *ACS Appl. Mater. Interfaces*, 2011, **3,** 1311; (c) J. Xu, W. S. Liu and Y. Tang, *Sci. China. Chem.*, 2013, **43**, 1272; (d) S. Banerjee, R. Kandanelli, S. Bhowmik and U. Maitra, *Soft Matter*, 2011, **7**, 8207; (e) B. Yan, *RSC Adv.*, 2012, **2**, 9304; (f) J. Feng and H. J. Zhang, *Chem. Soc. Rev.*, 2013, **42**, 387; (g) H. H. Zhang and H. R. Li, *J. Mater. Chem.*, 2011, **21**, 13576.

9 (a) R. Giustetto, F. X. L. Xamena, G. Ricchiardi, S. Bordiga, A. Damin, R. Gobetto and M. R. Chierotti, *J. Phys. Chem. B*, 2005, **109**, 19360; (b) J. Huang, Y. Liu, Q. Jin, X. Wang and J. Yang, *J. Hazard. Mater.*, 2007, **143**, 541.

10 H. Van Olphen, *Science*, 1966, **154**, 645.

11 (a) M. S. Augsburger, J. C. Pedregosa, E. Strasser, E. Perino and R. C. Mercader, *J. Phys. Chem. Solids*, 1998, **59**, 175; (b) M. José-Yacaman, L. Rendon, J. Arenas and M. C. Serra Puche, *Science*, 1996, **273**, 223; (c) A. Doménech, M. T. Doménech-Carbó, M. S. del Río, M. L. V. de A. Pascual and E. Lima, *New J. Chem.*, 2009, **33**, 2371.

12 (a) Y. F. Ma, H. P. Wang, W. S. Liu, Q. Wang, J. Xu and Y. Tang, *J. Phys. Chem. B*, 2009, **113**, 1413; (b) J. Xu, Z. Sun, L. Jia, B. Li, L. Zhao, X. Liu, Y. Ma, H. Tian, Q. Wang, W. Liu and Y. Tang, *Dalton Trans.*, 2011, **40**, 12909.

13 (a) T. Welton, *Chem. Rev.*, 1999, **99**, 2071; (b) P. Wasserscheid and W. Keim, *Angew. Chem., Int. Ed.*, 2000, **39**, 3772; (c) K. R. Seddon, *J. Chem. Technol. Biotechnol.*, 1997, **68**, 351.

14 (a) K. Binnemans, *Chem. Rev.*, 2007, **107**, 2592; (b) K. Lunstroot, P. Nockemann, K. Van Hecke, L. Van Meervelt, C. Görller-Walrand, K. Binnemans and K. Driesen, *Inorg. Chem.*, 2009, **48**, 3018; (c) K. Lunstroot, K. Driesen, P. Nockemann, C. Gorller-Walrand, K. Binnemans, S. Bellayer, J. Le Bideau and A. Vioux, *Chem. Mater.*, 2006, **18**, 5711.

15 S. Cousinié, M. Gressier, C. Reber, J. Dexpert-Ghys and M. J. Menu, *Langmuir*, 2008, **24**, 6208.

16 (a) P. Lenaerts, K. Driesen, R. Van Deun and K. Binnemans, *Chem. Mater.*, 2005, **17**, 2148; (b) L. N. Sun, J. B. Yu, H. J. Zhang, Q. G. Meng, E. Ma, C. Y. Peng and K. Y. Yang, *Microporous Mesoporous Mater.*, 2007, **98**, 156.

17 (a) W. P. W. Lai and W. T. Wong, *New J. Chem.*, 2000, **24**, 943; (b) L. N. Sun, S. Dang, J. Yu, J. Feng, L. Y. Shi and H. J. Zhang, *J. Phys. Chem. B*, 2010, **114**, 16393; (c) J. C. G. Bünzli and S. V. Eliseeva, *J. Rare Earths*, 2010, **28**, 824.

18 K. Binnemans, in: Handbook on the Physics and Chemistry of Rare Earths (ed.: K. A. Gschneidner Jr., J. C. G. Bünzli, V. K. Pecharsky), Elsevier, Amsterdam, 2005, vol. 35, chapter 225, 107.

19 (a) L. N. Sun, H. J. Zhang, L. S. Fu, F. Y. Liu, Q. G. Meng, C. Y. Peng and J. B. Yu, *Adv. Funct. Mater.*, 2005, **15**, 1041; (b) W. Q. Fan, J. Feng, S. Y. Song, Y. Q. Lei, L. Zhou, G. L. Zheng, S. Dang, S. Wang and H. J. Zhang, *Nanoscale*, 2010, **2**, 2096.

20 O. H. Park, S. Y. Seo, B. S. Bae and J. H. Shin, *Appl. Phys. Lett.*, 2003, **82**, 2787.

21 S. Comby, D. Imbert, C. Vandevyver and J. C. G. Bünzli, *Chem. - Eur. J.*, 2007, **13**, 936.

22 G. Boulon, A. Collombet, A. Brenier, T. Cohen-Adad, M. A. Yoshikawa, K. Lebbou, J. H. Lee and T. Fukuda, *Adv. Funct. Mater.*, 2001, **11**, 263.

23 (a) F. Wang, D. Banerjee, Y. S. Liu, X. Y. Chen and X. G. Liu, *Analyst*, 2010, **135**, 1839; (b) S. Comby and J. C. G. Bünzli, In Lanthanide near-infrared luminescence in molecular probes and devices, K. A. Jr. Gschneidner, J. -C. G. Bünzli, V. K. Pecharsky, ed. Handbook on the Physics and Chemistry of Rare Earths. Amsterdam: Elsevier Science B.V., 2007, 37, Ch. 235.

24 X. M. Guo, X. M. Wang, H. J. Zhang, L. S. Fu, H. D. Guo, J. B. Yu, L. D. Carlos and K. Y. Yang, *Microporous Mesoporous Mater.*, 2008, **116**, 28.

25 (a) X. Wen, M. Li, Y. Wang, J. Zhang, L. Fu, R. Hao, Y. Ma and X. Ai, *Langmuir*, 2008, **24**, 6932; (b) M. E. Hagerman, S. J. Salamone, R. W. Herbst and A. L. Payeur, *Chem. Mater.*, 2003, **15**, 443; (c) V. Martínez Martínez, F. López Arbeloa, J. Bañuelos Prieto and I. López Arbeloa, *J. Phys. Chem. B*, 2005, **109**, 7443.

26 K. Lunstroot, K. Driesen, P. Nockemann, K. V. Hecke, L. V. Meervelt, C. Görller-Walrand, K. Binnemans, S. Bellayer, L. Viau, J. L. Bideau and A. Vioux, *Dalton Trans.*, 2009, 298.

27 (a) K. Lunstroot, K. Driesen, P. Nockemann, L. Viau, P. H. Mutin, A. Viouxb and K. Binnemans, *Phys. Chem. Chem. Phys.*, 2010, **12**, 1879; (b) Y. Hasegawa, M. Yamamuro, Y. Wada, N. Kanehisa, Y. Kai and S. Yanagida, *J. Phys. Chem. A*, 2003, **107**, 1697.

28 H. Zhang, H. W. Song, H. Q. Yu, S. W. Li, X. Bai, G. H. Pan, Q. L. Dai, T. Wang, W. L. Li, S. Z. Lu, X. G. Ren, H. F. Zhao and X. G. Kong, *Appl. Phys. Lett.*, 2007, **90**, 103103.

29 H. Zhang, H. W. Song, B. Dong, L. L. Han, G. H. Pan, X. Bai, L. B. Fan, S. Z. Lu, H. F. Zhao and F. Wang, *J. Phys. Chem. C*, 2008, **112**, 9155.

30 (a) F. Liang, Q. Zhou, Y. Cheng, L. Wang, D. Ma, X. Jing and F. Wang, *Chem. Mater.*, 2003, **15**, 1935; (b) R. Reyes, M. Cremona, E. E. S. Teotonio, H. F. Brito and O. L. Malta, *Chem. Phys. Lett.*, 2004, **396**, 54; (c) J. Kido and Y. Okamoto, Chem. Rev.,2002, **102**, 2357; (d) L. H. Slooff, A. van Blaaderen, A. Polman, G. A. Hebbink, S. I. Klink, F. C. J. M. van Veggel, D. N. Reinhoudt and J. W. Hofstraat, *J. Appl. Phys.*, 2002, **91**, 3955.

31 (a) J. C. de Mello, H. F.Wittmann and R. H. Friend, *Adv. Mater.*, 1997, **9**, 230; (b) C. de Mello Donega, S. Alves, G.F. de Sá Jr., *Chem. Commun.*, 1996, **10**, 1199.

Efficient visible and near-infrared photoluminescent attapulgite-based lanthanide one-dimensional nanomaterials assembled by ion-pairing interactions

Efficient photoluminescent attapulgite-based one-dimensional lanthanide hybrid nanomaterials are first fabricated by ion-pairing interactions.